JOINT EUROPEAN TORUS JET

JET–P(87)15

P.H. Rebut and P.P. Lallia

JET Latest Results and Implications for a Reactor

JET Latest Results and Implications for a Reactor

P.H. Rebut and P.P. Lallia

JET-Joint Undertaking, Culham Science Centre, OX14 3DB, Abingdon, UK

Preprint of Paper presented at the 7th International Conference on Plasma Physics
Kiev, USSR 6th April - 10th April 1987

ABSTRACT

In nearly four years of operation of the JET tokamak, experiments have been undertaken with input powers up to 7MW of ICRF, ~10MW of neutral beam and ~18MW during combined operation. JET results show many advances made during this period. With ohmic heating alone, good confinement (τ_E up to 0.9s), high temperatures ($\hat{T}_e$ up to 5keV) and a fusion product $\langle \hat{n}_i \tau_E \hat{T}_i \rangle = 10^{20} m^{-3}.s.keV$ have been achieved. Highly efficient ion heating has been observed ($\hat{T}_i > 12.5 \pm 1.5$keV) at moderate neutral beam injection levels ($P_{NB} < 8$MW) and at low average densities ($\bar{n}_i = 1-1.5 \times 10^{19} m^{-3}$). But with increasing additional heating, confinement is degraded and thus additional heating has little impact on the fusion product. However, a fusion product of $2 \times 10^{20} m^{-3}.s.keV$ has been achieved with a magnetic separatrix configuration in JET. Experimental results are examined in terms of possible scaling laws for electron energy confinement and implications for a reactor are considered.

1. INTRODUCTION

The main objective of the Joint European Torus (JET) is to obtain and study plasmas in conditions and with dimensions approaching those needed for a fusion reactor (i.e. $n = 2 \times 10^{20} m^{-3}$; $T \geq 10$keV, and $\tau_E = 1-2$s). The aims of the JET project remain those set out at the start of the design phase in 1974, which were to study: (i) the scaling of plasma behaviour as plasma parameters approach the thermonuclear reactor regime; (ii) plasma-wall interactions in these conditions; (iii) plasma heating and (iv) α-particle production, confinement and consequential plasma heating.

The last item requires that the machine operates eventually in a deuterium-tritium mixture, and therefore, it has been designed for remote maintenance and tritium compatibility. The design, construction and operation of the machine were achieved by the dedicated efforts of the JET Team and the details have been reported, previously [1,2].

2. MACHINE STATUS

(a) Machine Conditions

Machine conditions have been progressively improved since first operation and all machine systems have now met or exceeded stringent design specifications. The achieved parameters are compared with the design values in Table I.

TABLE I

PRINCIPAL PARAMETERS OF JET: DESIGN AND ACHIEVED VALUES

PARAMETER	DESIGN VALUES	ACHIEVED VALUES
Plasma minor radius (horizontal), a	1.25m	0.8-1.2m
Plasma minor radius (vertical), b	2.10m	0.8-2.1m
Plasma major radius, R_o	2.96m	2.5-3.4m
Plasma elongation ratio, ϵ=b/a	1.68	1.2-1.7
Flat-top pulse length	Up to 20s	Up to 20s
Toroidal magnetic field (plasma centre)	3.45T	3.45T
Plasma current:		
circular plasma	3.2MA	3.0MA
Elongated plasma	4.8MA	5.1MA
Flux Drive Capability	34Vs	28Vs
Additional heating power (in plasma)	1986 Values / Full Values	
RF Power	8MW (3 antenna) / 32MW (8 antenna)	<7MW
Neutral beam power	10MW (1 box) / 20MW (2 boxes)	<9MW

In most recent experiments, eight carbon limiters have been located symmetrically on the outer equatorial plane of the vessel. Since disruptions mostly terminate on the inner walls, these have been covered by carbon tiles to a height of ±1m around the mid-plane. Similar tiles also protect the frames of RF antennae, eight octant joints and the outer wall from neutral beam shine-through. Additional tiles have been installed at the top and bottom of the vessel to protect the vessel during X-Point (separatrix) operation. The surface area covered (~45m^2) corresponds to ~20% of the vessel area. The inner wall tiles, used as limiters, and those for X-point protection have provided powerful pumping (with speeds up to 100mbar.l.s^{-1}), allowing operation at low densities near the plasma edge and were also used to reduce the density after neutral injection, to avoid disruptions. Recently, helium discharges prior to normal operation have improved the inner wall tiles pumping capacity.

(b) RF Heating System

Since early 1985, three RF antennae have been located at the outer equatorial wall. Power is transferred to the plasma at a radiation frequency (25-55MHz) corresponding to the cyclotron resonance of a minority ion species (H or He^3). Each antenna is fed by a tandem amplifier delivering up to 3MW in matched conditions. The three units have been regularly operated up to 7.2MW for 2s pulses. ICRF experiments with 8s pulse duration have delivered ~40MJ to the plasma.

(c) Neutral Beam System

A long pulse (~10s) neutral beam (NB) injector with eight beam sources and one integrated beam line system has been operated on JET since early 1986. H beams with particle energies up to 65keV and a total beam power of ~5.5MW have been injected into D plasmas. D beams with particle energies up to 75keV and a total power up to 10MW have also been injected into D plasmas. Up to 40MJ have been delivered to the plasma during a pulse.

(d) Diagnostics

About 30 different diagnostics have been installed on JET, allowing cross checking of the main plasma parameters and detailed analysis of the main plasma features. The details have been described, previously (3).

3. EXPERIMENTAL RESULTS

(a) Plasma Parameters

Three main modes of operation have been employed on JET, in which plasmas have been bounded by:

(i) eight carbon limiters on the outer equatorial plane;

(ii) carbon tiles on the inner equatorial plane (small major radius side of vacuum vessel);

(iii) a magnetic separatrix with X-points at the top and bottom of the torus.

In these configurations, various heating scenarios have been used, ranging from ohmic heating alone to combinations of ohmic, RF and NB. The main JET parameters achieved are presented in Table II. Examples of typical pulses under various conditions are indicated in Fig.1, which show the density (n), electron temperature (T_e) and safety factor (q) profiles, with ion temperature (T_i) measurements, where available.

Under these different conditions, plasma parameters have been obtained, as follows:

(i) with ohmic heating only, $\hat{T}_i$ and $\hat{T}_e$ of 3keV and 4keV, respectively, were achieved with $\bar{n}$ ~$4.2\times10^{19}m^{-3}$ and τ_E up to 0.9s;

(ii) with RF heating, $\hat{T}_i$ and $\hat{T}_e$ reached 5.5keV with $\bar{n}=3.5\times10^{19}m^{-3}$, however, τ_E dropped to ~0.3s. $\hat{T}_e$ reached 8keV in He plasmas;

(iii) with neutral beam heating, $\hat{T}_i$ up to 6.5keV at $n=3\times10^{19}m^{-3}$ was produced. At lower densities ($n\sim1.5\times10^{19}m^{-3}$), $\hat{T}_i \geq 12.5$keV was observed (Fig.1(e)). Again, degradation in τ_E to 0.3-0.4s was seen. With ~7MW of neutral beam injection, current drive of

TABLE II

SUMMARY OF MAIN JET PARAMETERS
(NOT NECESSARILY IN THE SAME PLASMA PULSE)

PARAMETER			VALUE
Safety factor at Plasma boundary	q_{cyl}	$\geq$	1.5
	q_ψ	$\geq$	2.1
Vol. average Electron density	$\bar{n}(x10^{19}m^{-3})$	$\leq$	5.0
Central electron temp.	$\hat{T}_e$(keV)	$\leq$	8.0
Central ion temp.	$\hat{T}_i$(keV)	$\leq$	12.5
Global energy conf. time	τ_E(s)	$\leq$	0.9
Fusion performance Parameters	$\langle \hat{n}_i \hat{T}_i \tau_E \rangle$ ($x10^{19}m^{-3}$.keV.s)	$\leq$	20.
Input ICRF power	P_{RF}(MW)	$\leq$	7.0
Input NBI power	P_{NB}(MW)	$\leq$	9.0
Total input power	P_t(MW)	$\leq$	18.0
Stored plasma energy	W_p(MJ)	$\leq$	6.1

0.4MA was observed at $n=2x10^{19}m^{-3}$;

(iv) 15MW of combined RF and NB heating was coupled to the plasma in a 5MA discharge: the plasma energy content was ~6MJ (Fig.1(d));

(v) in single null "X-point" discharges, H modes have been obtained. At 3MA and with 8MW of NBI, a plasma energy content of 6MJ has been observed.

The JET impurity behaviour is similar to that observed in other ungettered tokamaks with graphite limiters [4]. In most cases, impurity radiation losses were mainly caused by carbon and oxygen and originated mainly near the plasma edge. In limiter discharges, metal concentrations were only significant (i.e. >0.1% n_e) when the carbon limiters were metal-coated following accidental melting and evaporation of wall material. The release of metals from the limiters can be explained by a combination of sputtering by deuterium and by light impurities. The metal fluxes decrease as the plasma density increases and the plasma current decreases. These fluxes are inversely

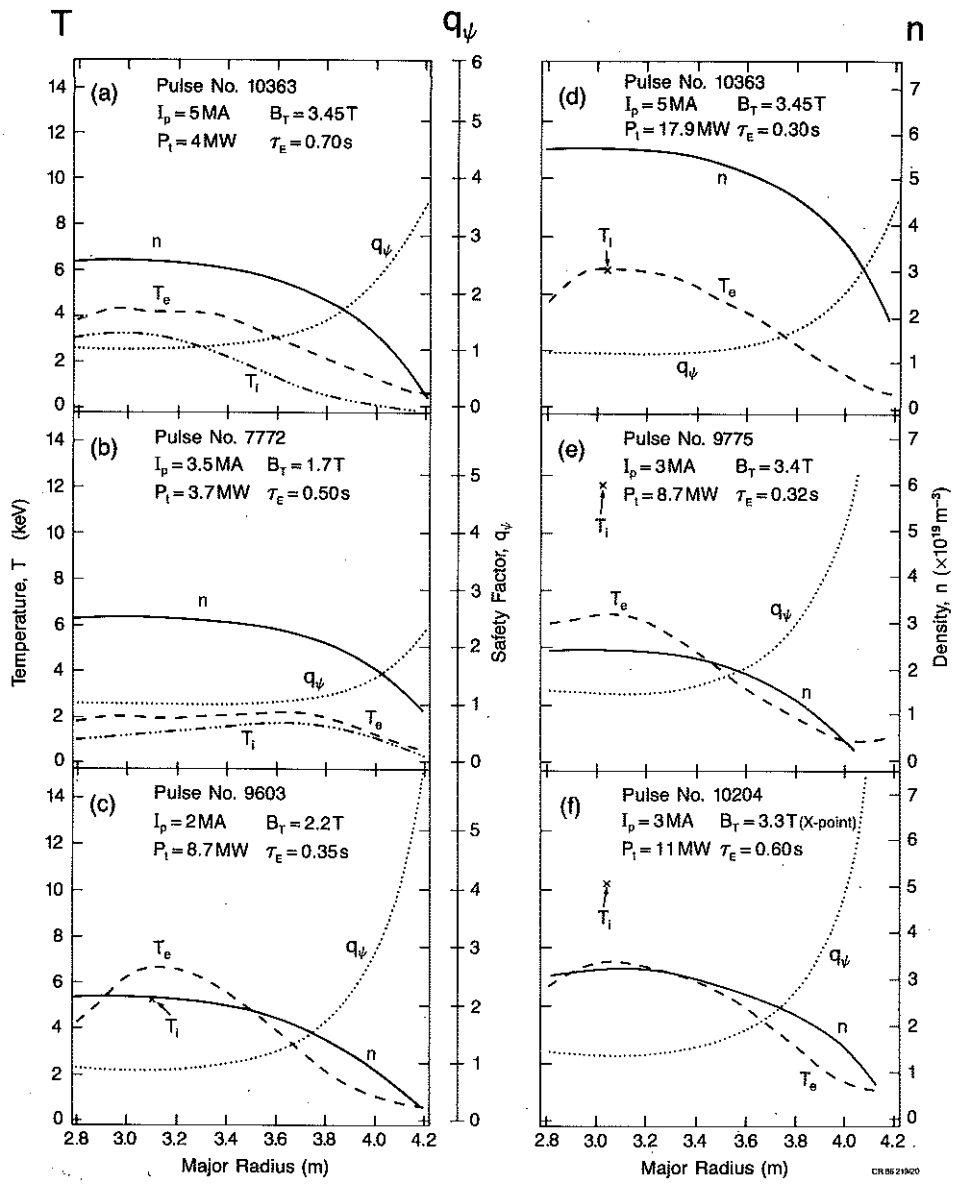

Fig.1 The density (n), electron temperature (T_e) and safety factor (q) as a function of major radius. The ion temperature (T_i) is shown where available. These profiles are indicated for the cases: (a) 5MA pulse (No:10363), Ohmic heating only, B_T=3.45T; (b) Low q pulse (No:7772), ohmic heating only, I_p=3.5MA, B_T=1.7T; (c) Monster sawtooth pulse (No:9603), P_{add}=6.1MW; (d) 5MA Pulse (No:10363) with 15.2MW of RF + NB power, B_T=3.45T; (e) High T_i pulse (No:9775) P_{add}=8MW; (f) X-Point configuration pulse (No:10204) I_p=3MA P_{add}=8.2MW;

correlated with the light impurity behaviour. At high plasma density, radiation losses were mainly caused by oxygen.

The effective plasma charge Z_{eff} ranges usually between 2 and 3 for $\bar{n}_e > 3 \times 10^{19} m^{-3}$. Z_{eff} was reduced and approached unity for a time duration exceeding 0.5s after injection of a deuterium pellet.

(b) Density Limitations

The operating diagram for JET is shown in Fig.2. For a given normalised current (1/q), there is a band of operating densities. Below a certain density, the discharge fails to breakdown, and above a critical density, the discharge is terminated by a disruptive instability. In ohmic plasmas, the density limit is $n_c(OH)(m^{-3}) = 1.2 \times 10^{20} B_T(T)/qR(m)$, and depends on plasma purity. In RF heated discharges, it is only slightly increased, possibly because the effect of extra power is cancelled by an impurity increase. In neutral beam heated plasmas, the limit is substantially increased (see Fig.2) to $n_c(NB)(m^{-3}) = 2 \times 10^{20} B(T)/qR(m)$. Switching off neutral beams at high density causes the plasma to disrupt, which indicates that the power input plays an important role in the disruption mechanism. Preliminary experiments with a single-shot pellet injector have also exceeded the OH density limit [5].

Density limit disruptions are always preceeded by an increase in the impurity radiation at the plasma edge [4], and a contraction of the electron temperature profile followed by the growth of coherent MHD activity (principally m=2, n=1). Alternative theoretical models predict that either the temperature profile contraction leads to an unstable current profile [6,7], or that the increased radiation losses at the q=2 surface lead to a thermal instability [8]. However, both effects might be involved. Both models predict growth of an m=2, n=1 island before the disruption. Both observations and theoretical considerations show that the central plasma density can be increased by deep fuelling.

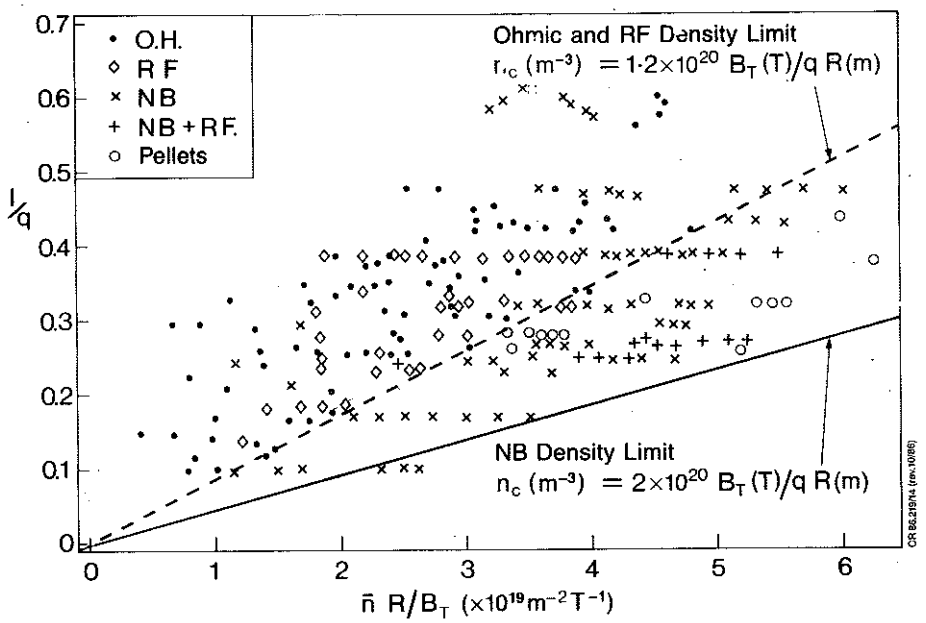

Fig.2 Normalized current [=1/q] versus normalised density [=$\bar{n}R/B_T$];

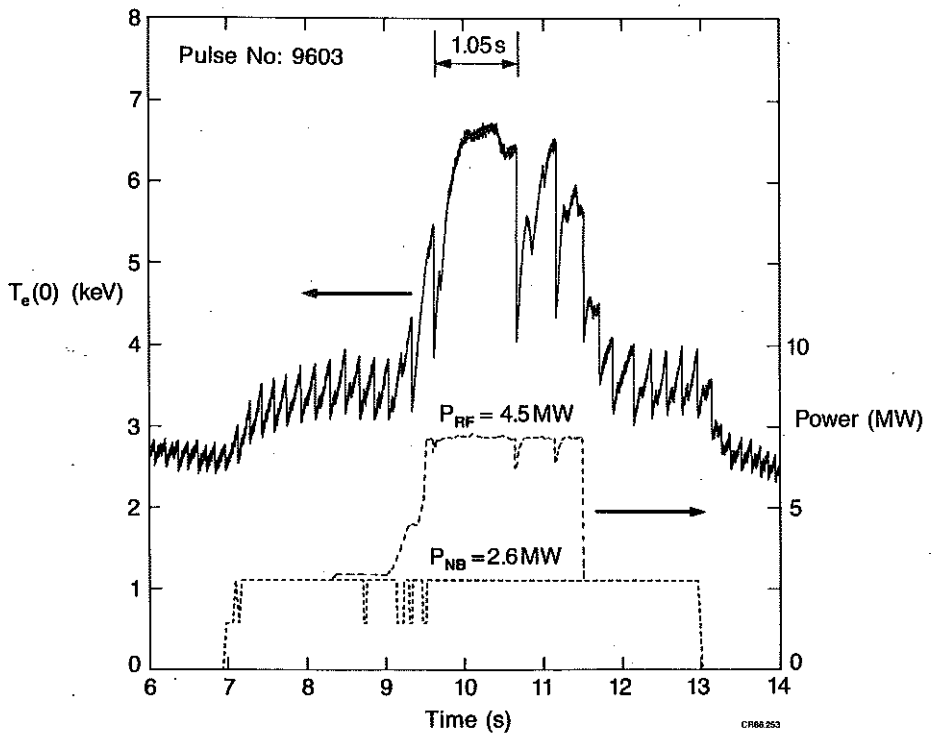

Fig.3 Sawtooth oscillations of the central electron temperature, showing the effects of NB and RF additional heating;

(c) Temperature Effects

Sawtooth oscillations are observed in most JET discharges. In general, these instabilities limit the T_e and T_i values, and in certain cases, the global energy confinement times. With central deposition of additional power, sawteeth may develop large amplitudes with up to 50% modulation in central electron temperature and long periods (up to 0.6s) [6]. In some cases, with NB and/or RF heating, 'monster' sawteeth have developed (see Fig.3), characterised by durations up to 1.6s and a strong reduction of the low m, n MHD activity.

The peak electron temperature $\hat{T}_e$ can be raised significantly with additional power above the value in the ohmic phase as shown in Fig.4(a). The dispersion seen in $T_e(0)$ is due to sawteething and to variations in profile deposition of the additional power. By contrast, the electron temperature at the inversion radius (q~1 surface) shows

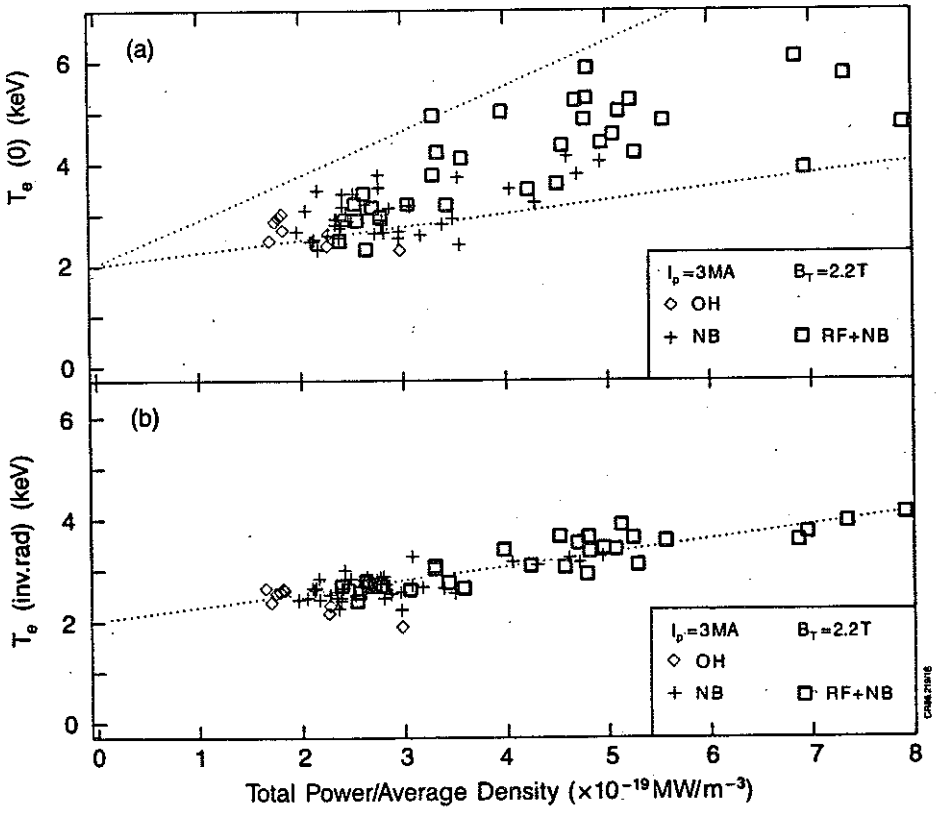

FIg.4 (a) electron temperature at the centre, (b) electron temperatures at the inversion radius (q=1);

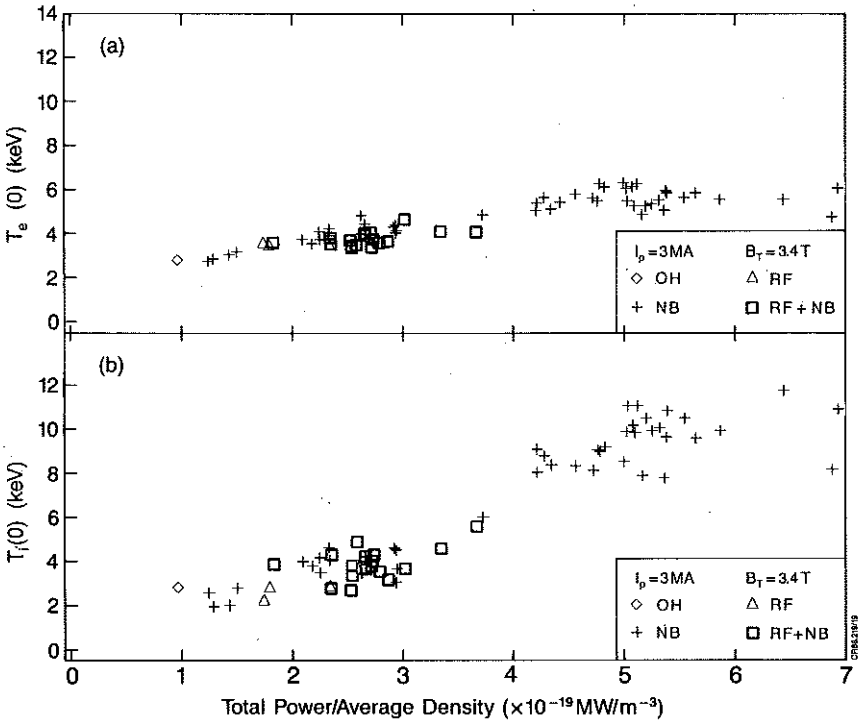

Fig.5 (a) electron temperature (T_e) at the centre and (b) ion temperature (T_i) at the centre as a function of power input per particle for various heating scenarios;

weak dependence with the power input per particle ($P/\bar{n}$) for a given plasma current and toroidal field (Fig.4(b)).

The ion temperature behaviour appears quite different; the peak ion temperature $\hat{T}_i$ is plotted in Fig.5(b) versus $P/\bar{n}$. Above 4×10^{-19}MW/m^{-3}, the ion temperature can greatly exceed the electron temperature and can reach ~12.5keV in JET.

(d) Confinement Degradation

The total energy confinement time on JET is defined by $\tau_E=W_k/[P_{tot}-dW_k/dt]$, where W_k is the kinetic energy and P_t is the total input power to the plasma without subtracting radiation losses. Reported values of τ_E are quasi-stationary.

With additional heating, the confinement time, τ_E, degrades with increasing input power (Fig.6(a)), as seen in a number of other experiments. The degradation is independent of type of heating,

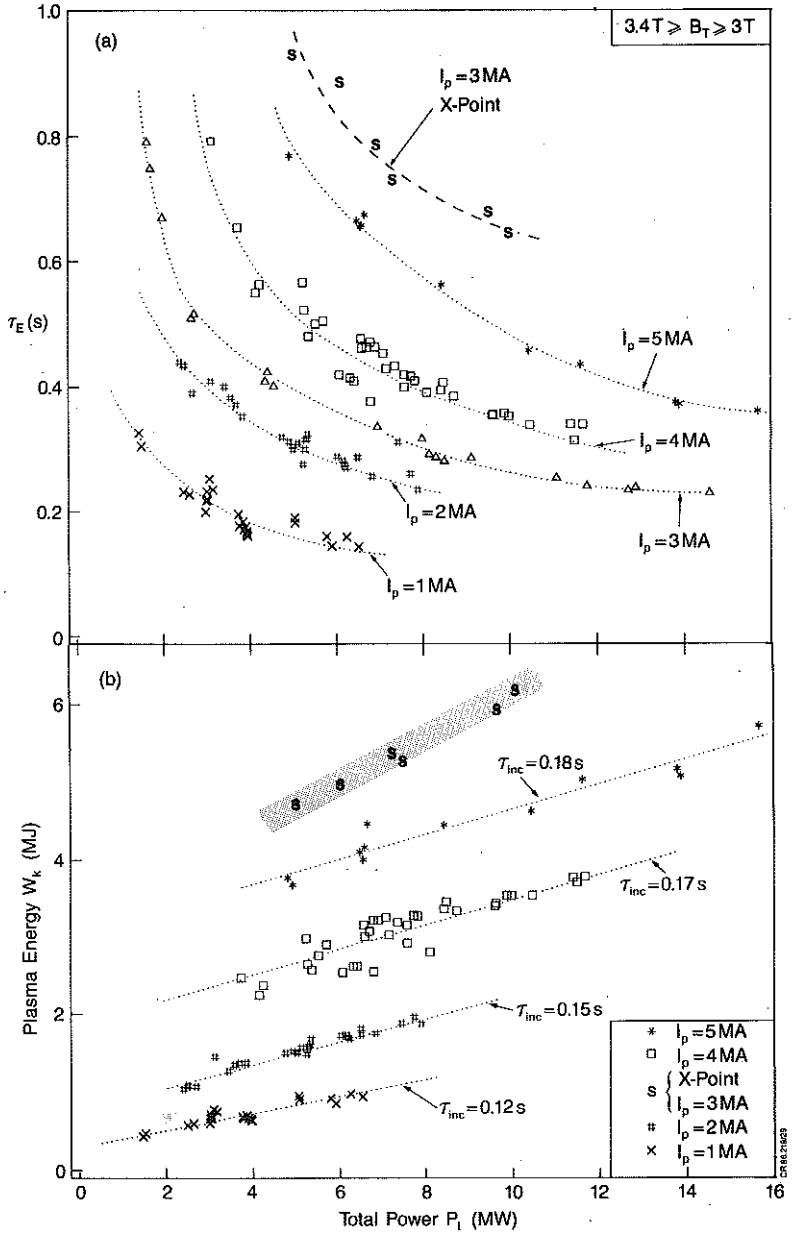

Fig.6 (a) the energy confinement time τ_E as a function of additional heating power (at I_p)=1,2,3,4 and 5MA; $3.4T \geq B_T \geq 3.0T$); (b) plasma energy content W_k versus the total input power P_t, with NBI or ICRF heating (I_p=1,2,4 and 5MA; $3.4T \geq B_T \geq 3.0T$);

whether RF, NB or combined. The rate of increase in W_k with $P_t (=\Delta W_k/\Delta P_t)$ appears to reach a limit of 0.1-0.3MJ/MW(=s) at high powers (see fig.6(b)), independent of type of additional heating. Confinement time depends weakly on plasma density but scales favourably with plasma current.

Since the plasma energy is a function of n_i, T_e and T_i, the degradation in confinement time is consistent with the observation that the electron temperature at the inversion radius (q=1 surface) increases little with power input (see Fig.4(a) and (b)).

(e) Magnetic Separatrix Experiments

A better confinement regime with additionally heated plasmas has been observed (H-mode) in some Tokamaks with magnetic limiters or divertors. Stable discharges with a magnetic separatrix (or X-point) inside the vessel have been maintained in JET for several seconds, at plasma currents up to 3MA with a single null and up to 2.5MA with a double null [9]. The single null discharges have an elongation of 1.65 (see Fig.7) compared with 1.80 for the double null and are therefore more stable against vertical displacements. In these configurations, the plasma is detached from both the limiter and the inner wall; recycling occurs in an open divertor region near the X-point. While interaction

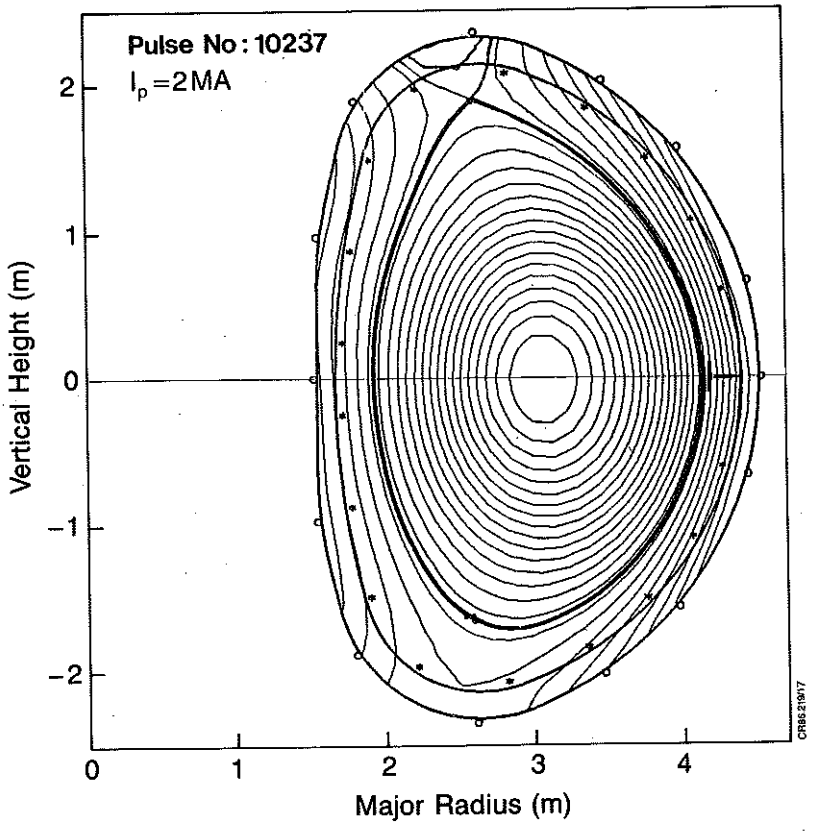

Fig.7 Single-Null X-Point configuration

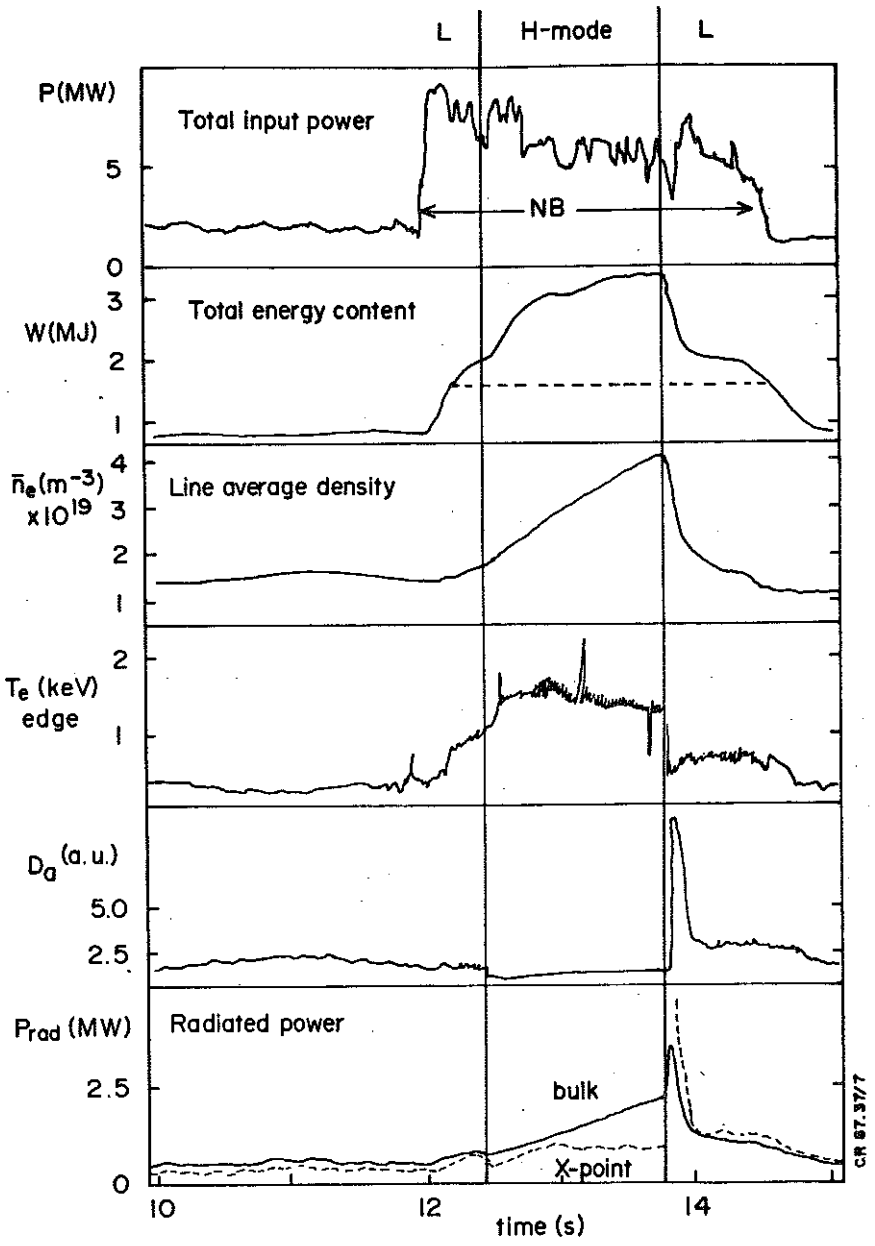

Fig.8 Single-Null X-Point experiment (Pulse No:10237) showing time evolution of:

(a) total input power, P_t;

(b) power to target plates (P_t-P_{rad}-dW/dt) (from bolometric analysis);

(c) total energy content W from the diamagnetic loop;

(d) line electron density, $\int n_e dl$;

(e) plasma edge temperature, T_e(edge);

(f) D_α signal from the plasma boundary.

of the discharges with the limiters was curtailed, the increased localised power deposition on the top and bottom target plates has, so far, limited the total input power to 10MW.

With neutral beam heating power greater than 5MW, a transition to enhanced plasma confinement (H-mode) was obtained in single null operation with B_T=2.2T. The usual H-mode features were observed (see Fig.8); decreased D_α light emission at the plasma boundary, reduced broadband magnetic fluctuations near the X-point, a rise in plasma density and in energy content, a sudden increase of electron temperature near the separatrix producing a pedestal to the temperature profile (see Fig.9b)and a flat density profile with a steep gradient near the separatrix (see Fig.9a). The H-mode phase could be sustained for durations approaching 2s. The continuous density rise increased the radiated power from the bulk plasma and is the likely cause for termination of this phase. There was no indication of a peaking of the impurity profile. While the energy content reached a quasi-steady state for times approaching 1s, the electron temperature could reach a maximum before the end of the H-mode phase. In these conditions, a plasma energy content of 6MJ was obtained with 8MW NB heating in addition to ohmic power of 2MW at I_p=3MA. The global confinement time in this mode exceeded by more than twice that value obtained with limiter or inner wall discharges. Increasing the magnetic field raised the power threshold required to switch to an H-mode, and has so far prevented a transition occurring with B_T>2.8T. H-modes have not yet been achieved with a double null configuration.

Separatrix operation appears to induce substantial changes in the plasma behaviour compared to limiter operation. This is possibly a result of the high shear at the boundary of the plasma, consistent with H modes obtained with a separatrix almost on the wall.

(f) Progress Towards Breakeven

A record value of the fusion product $\langle \hat{n}_i \tau_E \hat{T}_i \rangle$ of $2\times10^{20} m^{-3}.s.keV$ has been achieved with 10MW neutral beam heating during X-point operation

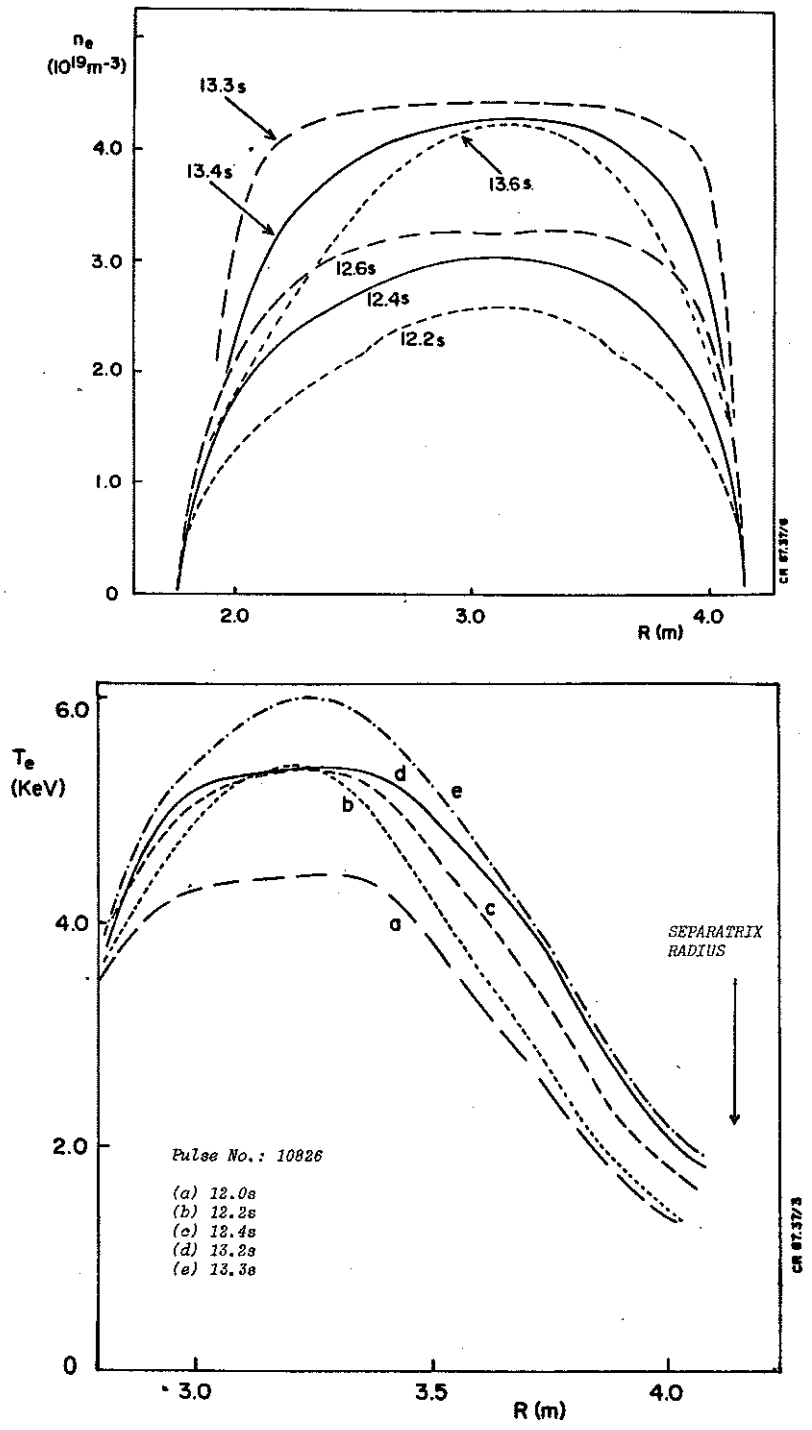

Fig.9 (a) Density profiles during L→H→L transition (times are marked on the diagram);
(b) Temperature profiles during L→H transition (times are marked on the diagram).

in the H-mode. For limiter discharges, the values of the fusion product are similar for ohmic, RF, NB and combined heating methods. This is caused by degradation in confinement time offsetting gains made in other parameters. The maximum values of the fusion product and the corresponding values of plasma temperature, density and energy confinement time are given in Table III for differing operating scenarios.

TABLE III

MAXIMUM VALUES OF $\langle \hat{n}_i \tau_E \hat{T}_i \rangle$

EXPERIMENTAL PROGRAMME	PEAK DENSITY $\hat{n}_i$ ($\times 10^{19} m^{-3}$)	ENERGY CONFINEMENT TIME τ_E (s)	ION TEMPERATURE $\hat{T}_i$ (keV)	FUSION PARAMETER $\langle \hat{n}_i \tau_E \hat{T}_i \rangle$ ($\times 10^{19} m^{-3}$.s.keV)	Q_{DT} EQUIVALENT Q_{DT}	PLASMA CURRENT I_p (MA)
Ohmic (4.6MW)	4.2	0.8	3.0	10	0.010	5
ICRF (7MW)	3.7	0.3	5.4	6	0.012	3
NBI (6MW)						
High n_i	4.4	0.4	4.0	7	0.10*	3
Low n_i	1.5	0.4	10	6	0.20*	3
Combined NBI + RF (14MW)	5.0	0.4	3.5	7	0.10*	3
X-point (NB-10MW)	5	0.65	6	20	0.15*	3

*Beam-Plasma reactions are dominant

Neutron yields up to $3 \times 10^{15} s^{-1}$ have been obtained with NB heating, mainly from deuterium-deuterium reactions occurring between the deuterium particles in the heating beams and the plasma. The best ratio of fusion power to input power obtained was $Q_{DD}=3.5 \times 10^{-4}$ which is equivalent to $Q_{DT}=0.2$, if tritium was introduced into the machine under

these conditions and would correspond to a fusion power production of above 1MW.

4. SUMMARY OF JET RESULTS

A summary of JET results is given, as follows:

(a) both ICRF and neutral beam (NB) injection methods are effective in delivering power into the JET plasma with the expected profile depositions. Large central electron and ion temperature increases have been observed; $\hat{T}_e$ and $\hat{T}_i$ have reached values of 7.5keV at densities of $3\times10^{19}m^{-3}$. At lower density ($\sim1.5\times10^{19}m^{-3}$), $T_i \geq 12.5$keV has been measured;

(b) with both these heating methods, the plasma energy has increased with input power. About 6MJ energy has been achieved in JET plasmas with ~18MW of total power input. However, the rate of energy increase with power ($\Delta W_k/\Delta P_t$) ~0.1-0.3s is smaller than the corresponding ohmic confinement times (τ_E~0.6-0.8s). The fusion product $\langle \hat{n}_i \tau_E \hat{T}_i \rangle$ has reached values exceeding $10^{20}m^{-3}$.s.keV, both in ohmic plasmas at 5MA and with additional heating: the degradation in confinement offsets the gains in density and temperature;

(c) a higher fusion product value of $2\times10^{20}m^{-3}$.s.keV has been obtained in the X-point configuration at lower current (~3MA). Values of $\tau_E \approx 0.6$-0.7s and $\hat{T}_i$ up to 10keV were achieved with neutron production $\sim3\times10^{15}ns^{-1}$ equivalent to a thermal $Q_{DT}=0.1$, the total Q_{DT} being ~0.15;

(d) in the central region (inside the inversion radius) between sawtooth collapses, additional heating is effective in increasing the plasma electron temperature (cf monster sawteeth);

(e) outside this region, electron heating is poor. The electrons seem to be the main energy loss channel, which appears related to confinement properties and not to the heating process;

(f) good prospects exist on JET for production of several MW of α-particle power at a value $Q_{DT}\approx1$;

(g) α-particle heating is expected to behave in a similar fashion to

other heating methods. Therefore, a reactor must either: (i) work at moderate currents with sophisticated control of the central region; or (ii) work at high currents without the need for complex control and additional heating.

5. AN INTERPRETATION OF CONFINEMENT AND CONSEQUENCES FOR A REACTOR

JET data have been used to assess the status of theoretical understanding of heat transport. Local fluxes have been derived from measurements and compared with presently available theoretical values. No acceptable agreement has yet been found [10]. Heuristic scaling laws can be derived by using dimensionless parameters [11,12,13]. Dimensionless parameters can be categorized into two groups.

(a) Shape Parameters: defined as ratios of two components of the same physical quantity and which describe either the geometry of the plasma (such as q; R/a; r/a; b/a; $r(\partial q/\partial r)$; $r(\nabla T/T)$ etc.) or its composition (i.e. m_e/m_i; n_e/n_i; T_e/T_i; Z_{eff}).

(b) Structural Parameters: constructed from different physical quantities. The relationships between the structural parameters reflect the underlying physics. When atomic processes, such as ionisation, line radiation and charge exchange are excluded, it is sufficient to introduce six structural parameters to describe a Tokamak plasma in a steady state; these are shown in Table IV. In this table, the subscripts t and p refer to the toroidal and poloidal component, respectively, η is the resistivity, v_s is the sound velocity, v_A the Alfven velocity, v_E the velocity at which energy flows out of the system, v_{th} the electron thermal velocity and v_{dia} the component of the diamagnetic drift velocity resulting from the temperature gradient. The other symbols have their normal meaning.

When quasi-neutrality exists, i.e. when the Debye length does not play a role, the parameters Γ and ζ are used only to define the collisions between charged particles. For instance, the Spitzer resistivity (η-$T^{-3/2}$) is defined by the relationship $\Delta = \zeta\Gamma^{-2}$. The parameter Φ is

TABLE IV

STRUCTURAL PARAMETERS DESCRIBING A TOKAMAK PLASMA

DESCRIPTION	PARAMETER
Ideal MHD	$\beta = \frac{P}{B^2_t/2\mu_o} = (\frac{v_s}{v_A})^2$
Resistive MHD	$S = \frac{B_p v_A}{\eta j} = \frac{v_A}{v_{pinch}}$
Power flux balance	$\Phi = \frac{\text{Power flux}}{\text{Energy density x } v_s} = \frac{v_E}{v_s}$
Finite Larmor radius or two-fluid MHD	$\Omega = \frac{2m_e kT_e}{e^2 B^2_t r^2} = (\frac{v_{dia}}{v_{th}})^2$
Relativistic effects	$\Gamma = 2kT/m_e c^2 = (\frac{v_{th}}{c})^2$
Granular effects	$\zeta = e^2/rm_e$

required by the fact that the system is an open one: a continuous flow of energy to the plasma is provided by the various heating systems. Here only the dependence between structural parameters will be considered. This means that the expressions given in the following must be multiplied by a shape parameter function, which may not necessarily be known. Note that the magnetic Reynolds number S and Φ are ratios of velocities, while β and Ω are ratios of the square of velocities. In any relation between these parameters, it is anticipated that Φ and S will be affected by integer exponents, while β and Ω will be at a half power exponent. Also, the relationship between structural parameters should be relatively simple. Other well known dimensionless plasma physics parameters can be written in terms of previous ones. For instance, the drift parameter ($=j/env_{th}$) is $\xi = \Omega^{1/2}/\beta$.

The power balance equation with ohmic heating only is $\Phi_\Omega = 1/S\beta^{3/2}$ while the classical and neoclassical perpendicular transport are

described by $\Phi_{\perp} = \beta^{1/2}/S$ and the plateau regime by $\Phi_p = \Omega$. Parallel transport would be described by $\Phi_{\parallel} = \Omega S/\beta^{1/2}$.

The JET experimental results (in particular, the behaviour of the electron temperature profile) strongly suggest that there is no fundamental difference between ohmic and auxiliary heated discharges: the mechanisms responsible for confinement degradation already seem at work during the ohmic phase. A formulation of the electron radial heat flux ϕ_e, reflecting this behaviour could be:

$$\phi_e = n\chi_{an}\nabla T.g\left(\left|\frac{\nabla T}{(\nabla T)_c}\right|\right) + \phi_{neo}$$

where χ_{an} is the anomalous heat diffusivity responsible for the observed incremental confinement time and g is a function of the temperature gradient which goes to zero when ∇T is smaller than a critical value $(\nabla T)_c$. ϕ_{neo} reflects the neoclassical transport and is only significant when g=0. A possible form for g is:

$$g = \left[1 - \frac{(\nabla T)_c}{\nabla T}\right] \cdot H\left[\left|\nabla T\right| - \left|\nabla T\right|_c\right]$$

Such a form of the function g is supported by the JET results[14].

One hypothesis proposed is that $(\nabla T)_c$ corresponds to the establishment of a chaotic magnetic topology involving small islands [15]. The resulting flow of energy should then be a combination of parallel and perpendicular transport. Written in terms of dimensionless parameters, this means

$$\Phi_{an} = \Phi_{\perp}^{u} \cdot \Phi_{\parallel}^{v} \qquad \text{with } u + v = 1$$

The simplest form is u=v=½ and correspondingly, $\Phi_{an} = \left[\frac{\beta^{1/2}}{S} \cdot \frac{\Omega S}{\beta^{1/2}}\right]^{1/2} = \Omega^{1/2}$. Note that, except for missing shape parameters, this relation shows a sort of Bohm like diffusivity.

The expression for the critical electron temperature gradient should be deduced from the mechanism sustaining the perturbed magnetic topology. A non-proven but plausible one involves a balance between the pressure exerted on the islands, either by an acoustic wave (Ω_{c1}) or by a torsional Alfven wave (Ω_{c2}), and the resistive dissipation of the induced currents. In terms of dimensionless parameters, it reads

$$\Omega_{c1} = 1/S\beta^{3/2}$$

$$\text{or} \quad \Omega_{c2} = 1/S\beta$$

The heat flux equation becomes

$$\Phi = \left[\Omega^{1/2} - \Omega_c^{1/2} \right] H(\Omega - \Omega_c) + \text{Neo-classical terms}$$

Another term may enter the right side of equation when describing the boundary of the discharge where atomic physics becomes dominant.

With the help of empirical scaling of JET results [16], it has been possible to deduce some but likely not all the involved shape parameters and to propose here a heuristic scaling. The global electron energy content W_e can be deduced from the flux equation by solving for temperature and introducing the total input power, P_t, independent of the heating method (ohmic, NBI or ICRF).

$$W_e = \alpha_1 Z^{1/4} n^{3/4} B^{1/2} I^{1/2} L^{11/4} \left\{1 + \alpha_2 \frac{M^{1/2} P_t}{n^{1/2} Z^{1/2} B L^{3/2}}\right\}^{1/2} \qquad (1)$$

where the critical temperature gradient is defined by $\Omega_{c1} = 1/S\beta^{3/2}$; M is the atomic number, Z the effective charge, n the volume averaged density ($10^{19} m^{-3}$), I the plasma current (in MA), B the toroidal field (in T) and L an average size of the plasma (in m): ($L = \sqrt[3]{Rab}$). The coefficients α_1 and α_2 are found by a regressional fit on about 1,200 JET "limiter" data points. The result is $\alpha_1 = 2.3 \times 10^{-2}$ and $\alpha_2 = 3.0$ when W_e is in MJ and P_t in MW.

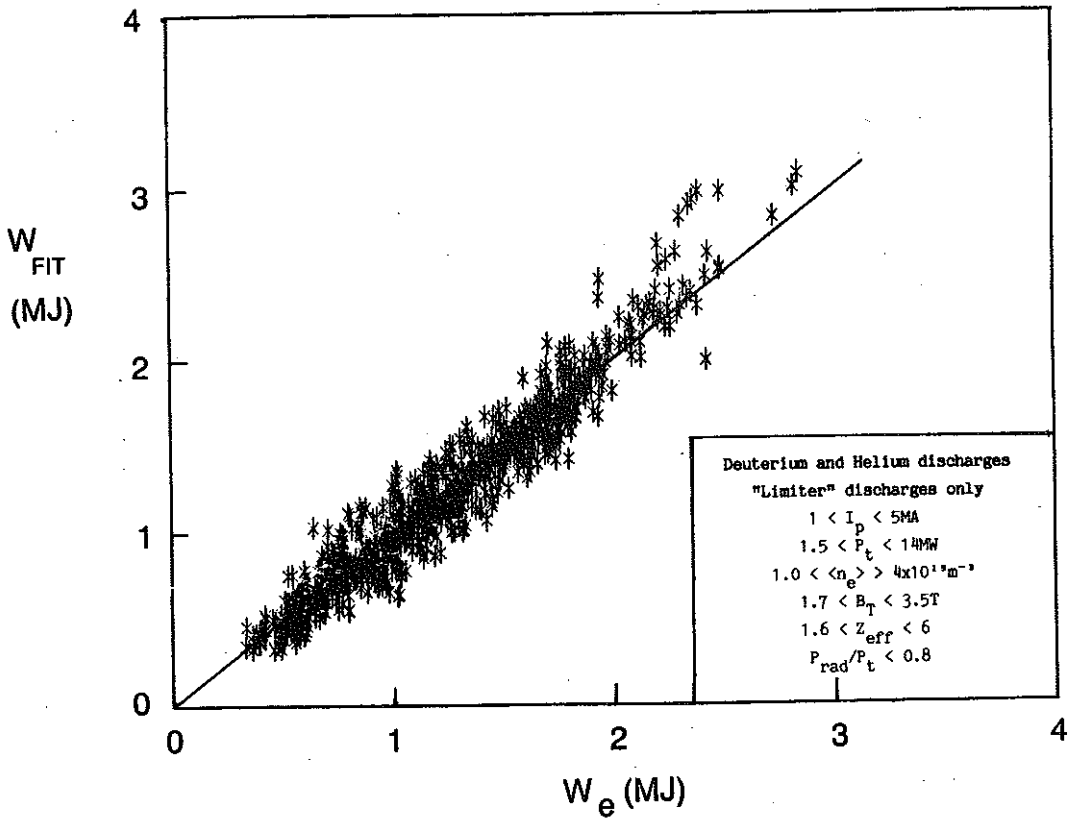

Fig.10 Total stored electron energy W_e versus the fit proposed in Eq.(1). Data include ohmic heating only, NBI only, ICRF only and combined heating.

The comparison between the fitted and calculated values is shown in Fig.10, where the range of the experimental data is indicated. While the JET plasma size is almost unchanged in all the data presented and some shape factors are still likely to be missing, the scaling provides the size dependence and fits quite well the results of smaller Tokamaks where the electron energy content is four orders of magnitude smaller.

If proven to be correct, the scaling proposed has direct consequences on the ignition margin and on the size of future devices. Note that the critical electron temperature, would vary as $(BI^2)^{1/4}$ at the density limit ($n \propto B/L$). As any increase above the critical temperature is very consuming in input power, it seems better to be close to the required ignition temperature already in the ohmic heating phase. A current and size increase in a Tokamak machine could achieve ignition without additional heating. The resulting simplification of

the overall system could well compensate for the larger size. The above scaling suggests that in a Tokamak with a major radius of ~x2.5 that of JET, a magnetic field close to 4.5T and a plasma current near 25MA, a deuterium-tritium plasma would ignite with ohmic and α-particle heating only. The thermonuclear output of such a machine could be increased by injecting fuel pellets: the thermal insulation should degrade as the additional heating provided by the α-particles increased without a strong variation of temperature. Burn control would be performed entirely through density control.

ACKNOWLEDGEMENTS

The JET achievements are the result of the work of the JET Team. In addition, we are pleased to acknowledge the help of Dr. K. Thomsen in handling the JET data resulting in Fig.10 and of Dr. B. Keen in reading carefully the manuscript.

7. REFERENCES

(1) Design, Construction and First Operational Experience of JET, Special Issue of Fusion Technology, 11, 43, (1987);

(2) P.H. Rebut et al, Proceedings of the 11th IAEA Conference on Plasma Physics and Controlled Nuclear Fusion Research (Kyoto, Japan, November 1986);

(3) P.E. Stott, Proceedings of the Workshop on High Temperature Plasma Diagnostics (Varenna, Italy, September 1986);

(4) K. Behringer et al, Proceedings of the 11th IAEA Conference on Plasma Physics and Controlled Nuclear Fusion Research (Kyoto, Japan, November 1986);

(5) A. Gondhalekar et al, Proceedings of the 11th IAEA Conference On Plasma Physics and Controlled Nuclear Fusion Research (Kyoto, Japan, November 1986);

(6) D.J. Campbell et al, Proceedings of the 11th IAEA Conference on Plasma Physics and Controlled Nuclear Fusion Research (Kyoto, Japan, November 1986);

(7) J.A. Wesson et al, Proceedings of the 11th IAEA Conference on Plasma Physics and Controlled Nuclear Fusion Research (Kyoto, Japan, November 1986);

(8) P.H. Rebut and M. Hugon, 10th IAEA Conference on Plasma Physics and Controlled Fusion Research (London, U.K.), (1984) Vol.II, p197;

(9) A. Tanga et al, Proceedings of the 11th IAEA Conference on Plasma Physics and Controlled Nuclear Fusion Research (Kyoto, Japan, November 1986);

(10) D.F. Düchs et al, Proceedings of the 11th IAEA Conference on Plasma Physics and Controlled Nuclear Fusion Research (Kyoto, Japan, November 1986);

(11) B.B. Kadomtsev, Fiz Plazmy, 1, (1975) 531; [Sov. Phys.-J. Plasma Phys., 1 (1975 295];

(12) J.W. Connor and J.B. Taylor, Nuclear Fusion, 17 (1977) 1047;

(13) P.H. Rebut and M. Brusati, Plasma Physics and Controlled Fusion, 28, 113 (1986);

(14) J.D. Callen, J.P. Christiansen, J.G. Cordey, P.R. Thomas and K. Thomsen, Modelling of Temperature Profiles and Transport Scaling in Auxiliary Heated Tokamaks, to be published in Nuclear Fusion, and N. Lopes Cardozo, this Conference;

(15) P.H. Rebut, M. Brusati, M. Hugon and P.P. Lallia, 11th IAEA Conference on Plasma Physics and Controlled Nuclear Fusion Research (Kyoto, Japan, November 1986) and M. Hugon et al, this Conference:

(16) J.G. Cordey et al, Proceedings of the 11th IAEA Conference on Plasma Physics and Controlled Nuclear Fusion Research (Kyoto, Japan, November 1986).